Rubber-Like Thermosetting Epoxy Asphalt Composites Exhibiting Atypical Yielding Behaviors

Yang Kang,[1] Zhiming Chen,[1] Zhen Jiao,[1] Wei Huang[2]

[1]*School of Chemistry and Chemical Engineering, Southeast University, Nanjing 211189, People's Republic of China*
[2]*College of Transportation, Southeast University, Nanjing 210096, People's Republic of China*

Received 1 June 2009; accepted 4 October 2009
DOI 10.1002/app.31563
Published online 5 January 2010 in Wiley InterScience (www.interscience.wiley.com).

ABSTRACT: Rubber-like thermosetting epoxy asphalt composites (REACs) were prepared by curing epoxy resin (diglycidyl ether of bisphenol A) with curing agents system made up of maleated petroleum asphalt, adipic acid, and methylhexahydrophthalic anhydride. REACs' glass transition temperatures (T_g) and mechanics performances were investigated by differential scanning calorimetry (DSC) and universal tester, respectively. DSC results indicated that REACs had homogeneous phase structures, and their T_g were lower than room temperature. Large elongation at break (ε_b), as high as 150–286%, and atypical yielding behaviors similar to so-called "hard elastic" thermoplastics were observed simultaneously for the first time as to thermosetting epoxy composites at room temperature. The striking characteristics of REACs were ascribed to the formation of unique asphalt-filled bimodal networks, consisting of simultaneous cured maleated asphalt short-chain and dicarboxylic acid long-chain interpenetrating bimodal networks and wherewith filled unmaleated asphalt. The experimental results suggest that these inexpensive REACs may find promising applications in many engineering fields. © 2010 Wiley Periodicals, Inc. J Appl Polym Sci 116: 1678–1685, 2010

Key words: epoxy; asphalt; thermosets; mechanical properties; interpenetrating networks (IPN)

INTRODUCTION

Epoxy resins are used widely in thermosetting materials because of their good mechanical, thermal, and electrical properties. To further strengthen the properties of epoxy resins, especially to toughen epoxy resins, many methods have been developed, such as modifying with an additional phase,[1,2] usage of flexible curing agents,[3,4] forming interpenetrating networks with thermoplastics.[5,6] These modifications have improved epoxy resin's toughness to some extent. On the other hand, asphalt is a typical viscoelastic and thermoplastic material. At high temperature, the viscous properties dominate and the asphalt tends to flow, whereas at low temperature, the elastic properties dominate and the asphalt tends to resist flow. Wherefore, its applications are restricted by the temperature sensitivity, which reflects the thermoplastic nature of asphalt. To avoid the temperature sensitivity, kinds of modification methods including physical coblends[7–11] and chemical modifications[12–14] have been developed. Although the adoption of these methods results in somewhat improvement of the asphalt properties, the corresponding modified asphalts were also thermoplastic in essence.

It is attractive to combine two different materials into one composite to simultaneously avoid thermoplastic nature of asphalt and brittleness of epoxy resin. Thermosetting epoxy asphalt composites (EACs)[15–21] have been broadly investigated in last 3 decades. Nevertheless, epoxy resin and the asphalt tend to separate from each other due to their poor compatibility. The EACs are brittle glassy composites at room temperature; in other words, they are not elastic or rubber like. However, rubber-like thermosetting composites usually imply composites related to polyurethane,[22–24] and rubber-like thermosetting EAC (REAC) was almost not reported.

To prepare stable REACs, we conceive that first modifying the common used petroleum asphalt with maleic anhydride (MAH)[25–27] to obtain the maleated asphalt, which can be cured by the epoxy resin so as to improve the compatibility of asphalt and epoxy resin, and hence, avoiding the asphalt bleeding from the curing product at the most extent. Moreover, the maleated asphalt could present many short chains that would enhance the cured composites' intensity, according to the bimodal networks theory.[28–30] Afterward, adipic acid (AA) and methylhexahydrophthalic anhydride (MeHHPA) are added as long-chain

Correspondence to: Z. Chen (chenzm@seu.edu.cn).
Contract grant sponsor: Nation High tech R&D Program (863 Program, P R China); contract grant number: 2007AA03Z562.
Contract grant sponsor: Industrialization Funds for Sci&Tech Achievements (Jiangsu Province, P R China); contract grant number: BA2007105.

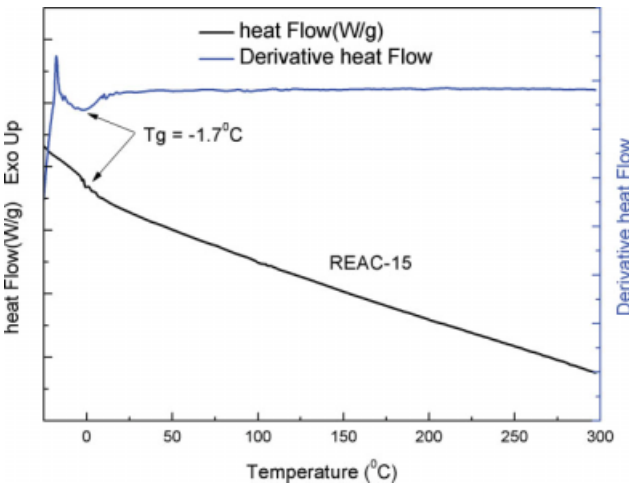

Figure 1 DSC and its differential coefficient curves of REAC-15. [Color figure can be viewed in the online issue, which is available at www.interscience.wiley.com].

flexible epoxy curing agents to increase the elongation and tensile strength of the cured REACs.

EXPERIMENTAL

Materials

Maleic anhydride (MAH, Wuxi Resin, Wuxi, China), adipic acid (AA, Yongzai Chemical, Zhejiang, China), methylhexahydrophthalic anhydride (MeHHPA, Guanghui Hitech Chemical, Changzhou, China), Asphalt (90#, Shell, China), and epoxy resin (E-51, diglycidyl ether of bisphenol A, Wuxi Resin, Wuxi, China) were used as received.

Preparation of component A

Reactions were carried out in a wide-mouthed glass flask fitted with a mechanical stirrer, a condenser (warm water refluxing, 75–85°C), a gas inlet for N_2 purge, and a thermocouple. First, MAH was added into the flask loaded with 150°C asphalt (4 : 100, wt.). It was stirred for 4–6 h keeping the temperature to carry out the maleation reaction of asphalts. Then, AA and MeHHPA (10 : 1, wt.) were poured into the flask subsequently. Finally, mixture was agitated for about 0.5 h, and N_2 was purged for 1 h. The end product was designated as component **A** and the epoxy resin E-51 as component **B**. Control experiments were carried out as above in the absence of MAH or asphalt, respectively.

Characterization and measurement

Direct tensile

Component **A** and **B** were heated to 120°C, mixed and sheared for 1 min, and then, the mixture was poured into heated (120°C) mold and baked (120°C) in an oven to cure for 4 h. The cured REAC was demoulded and cooled to room temperature (23°C). The uniaxial tensile test was carried out using a WDW-2000 Universal Tester (Changchun Kexin Test Machine, China) according to ASTM D638.

Differential scanning calorimetry

To determine the glass transition temperature, which was obtained from the midpoint of the endotherm of differential scanning calorimetry (DSC) curve or peak of the derivative heat capacity vs. temperature curve,[31] a TA DSC Q 10 was used. Approximately 10–20 mg of sample, after uniaxial tensile test, was placed into a sealed alumina crucible and put inside the furnace under a blanket of nitrogen purging at a rate of 20 mL min^{-1}. The temperature was increased to 300°C from −50°C at a rate of 10°C min^{-1}.

Fluorescence microscope

Fluorescence microscope (CFM-300E, Shanghai Changfang Optical Instruments, Shanghai, China) was used to observe the microstructure of component **A**.

RESULTS AND DISCUSSION

Glass transition

As shown in Figure 1, REAC has only one glass transition temperature (T_g) in the range of −30 to 300°C. Figure 2 shows that with the increase of $C_{\text{maleated asphalt}}$ (maleated asphalt content of component **A**), REAC's glass transition temperature (T_g) increases because the maleated asphalt as the short chain curing agents of epoxy resins results in higher

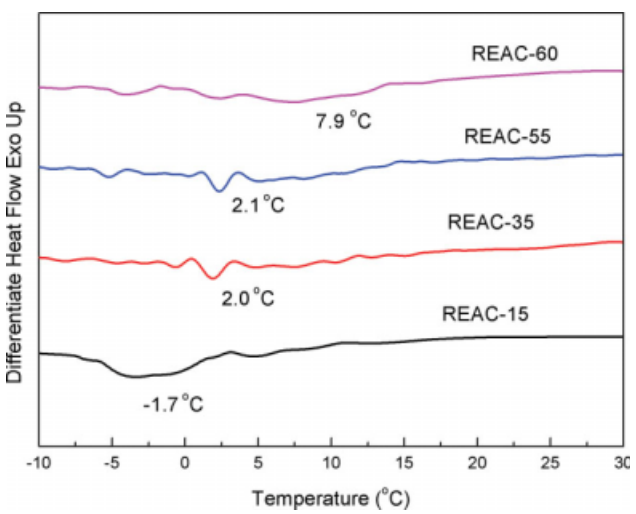

Figure 2 Differential of DSC curves. [Color figure can be viewed in the online issue, which is available at www.interscience.wiley.com].

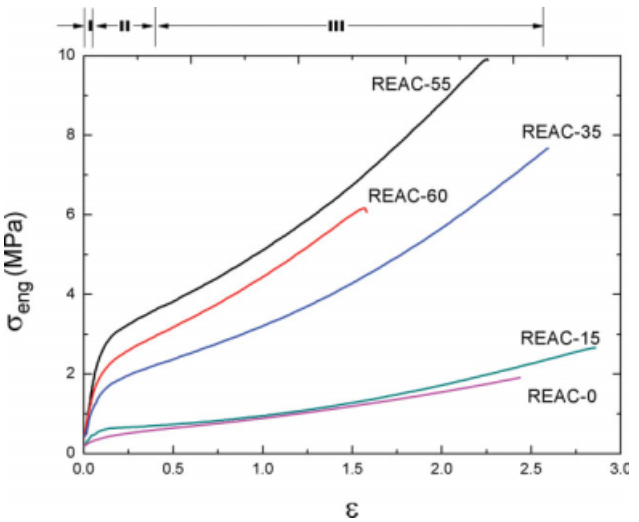

Figure 3 Stress–strain curves of REACs. [Color figure can be viewed in the online issue, which is available at www.interscience.wiley.com].

crosslinking density of the cured REACs. The sharp peaks of T_g indicate that maleated asphalt and epoxy have good compatibility, which means maleation effectively avoid asphalt bleeding from the cured REACs, as we conceived. Also, T_g of every REACs, which is below room temperature, reveals that REACs are homogeneous and rubber-like materials.

Mechanics

Tensile strength and Young's modulus

As shown in Figures 3 and 4 and Table I, REACs exhibit striking mechanical properties in two aspects. One is the large elongation at break (ε_b), as high as 150–280%, and the other is the atypical yielding behavior.

Figure 3 shows typical stress–strain curves for REACs with different maleated asphalt contents of component **A**. REAC-15 exhibited a high ε_b of 286%. (Here, the sample codes for REACs were defined by $C_{\text{maleated asphalt}}$, e.g., REAC-15 when $C_{\text{maleated asphalt}}$ is 15 wt %). It is the highest value ever reported for conventional asphalt or modified asphalt and epoxy composites. The stress–strain curves varied greatly depending on $C_{\text{maleated asphalt}}$, as shown in Figure 3, whereas the general features of the curves were similar for all REACs. The Young's modulus (E_i) and ultimate tensile strength (σ) increased evidently (Table I) with $C_{\text{maleated asphalt}}$. It should be noted that the fracture energy ($J = \int_0^{\varepsilon_b} \sigma d\varepsilon$, used to characterize materials' toughness[32]) of REAC-55 was as many as five times higher than that of the REAC-0 (especially, REAC-0 was cured at 120°C for 8 h, whereas others were cured at 120°C for 4 h).

Moreover, the stress–strain curves have no evident yield point and upturns at the last tensile stage, which are different from conventional rubber-like ones. The atypical yielding behavior of REACs was accompanied by high elongation, which is evident in both the stress–strain curve (Fig. 3) and direct observation (Fig. 4). Furthermore, tensile test indicated that REACs had large deformation and no-necking phenomena like rubbers and had times higher Young's modulus than rubbers. (According to ASTM's definition, rubbers' Young's modulus are of 1–10 MPa).

In previous studies of material mechanical properties, similar yielding behavior and associated no-necking phenomena were observed for many polymeric materials so-called "hard-elastic materials," such as PP,[33] PE,[34] PVDF,[35] or HIPS[36] prepared by special technique. However, in all cases, they were thermoplastic. Thus, for the thermosetting epoxy composites, it is reported for the first time that thermosetting REACs have atypical yielding (and no-necking) and large elongation simultaneously, distinguishing them from previous materials.

In this regard, the stress–strain curve was divided into three regions (Fig. 3). The first section (I) is an initial linear-elastic region with high modulus. The second (II) is an interim region. The third (III) is a large deformation region at almost constant rate of stress that starts from the end of interim, which looks like another linear-elastic region. The characteristic mechanical behavior was observed from all REACs with different $C_{\text{maleated asphalt}}$, although it was more distinctive in REACs with $C_{\text{maleated asphalt}} > 15$ wt % (Fig. 3). For most of REACs, the interims' strains were observed at about 3–15%, whereas the ε_b and σ exhibited a strong dependence on $C_{\text{maleated asphalt}}$ (Fig. 3). With $C_{\text{maleated asphalt}}$, REACs' ε_b and σ were simultaneously improved (Fig. 3) because local density of crosslinking networks were increased by the short chains maleated asphalt; however, when $C_{\text{maleated asphalt}}$ was higher than a threshold, the higher local density of crosslinking networks would increase the global density of crosslinking networks, and thus, the REAC's mechanical performance impaired, as shown in Figure 3 (REAC-60). That is,

Figure 4 Images of tensile behavior of REAC-55. [Color figure can be viewed in the online issue, which is available at www.interscience.wiley.com].

TABLE I
Mechanical Properties of REACs

	Sample				
	REAC-60	REAC-55	REAC-35	REAC-15	REAC-0
Cure condition	4 h at 120°C	4 h at 120°C	4 h at 120°C	4 h at 120°C	8 h at 120°C
Tensile strength (MPa)	6.13 ± 0.5	9.87 ± 0.8	7.67 ± 0.4	2.85 ± 0.2	1.92 ± 0.1
Rupture elongation (%)	156.2 ± 6.3	226.1 ± 7.1	259.4 ± 8.0	286.0 ± 9.2	243.4 ± 7.5
Young's Modulus (MPa)	81.9 ± 1.3	85.8 ± 1.3	75.7 ± 0.9	36.5 ± 0.5	34.5 ± 0.5

all the REACs' mechanics are consistent with the judgments of bimodal networks theory.[28–30]

Compared with these observations, REAC-0 with the composition corresponding to REAC-55—except for the unmaleated asphalt instead of the maleated asphalt—was soft and broken at relative low elongation, as shown in Figure 3. Also, epoxy resin E-51 cannot be cured by the component **A** corresponding to REAC-55 without asphalt at 120°C for over 12 h. REACs could withstand high levels of deformation not only in uniaxial elongation as described above but also in other deformations, such as compression, tearing, and bending.

Elongation

To clarify the nature of the high elongation, strain–stress curves were investigated in virtue of rubber-likes' phenomenological model. Although many refinements[37–39] have been developed to describe the stress–strain behavior of rubber-likes, Mooney–Rivlin representation is the most popular form used to discuss rubbers' stress–strain curves.[40–42]

$$\frac{\sigma_{eng}}{\lambda - 1/\lambda^2} = 2C_1 + \frac{2C_2}{\lambda}$$

The reduced stress $\frac{\sigma_{eng}}{\lambda-1/\lambda^2}$ is a linear function of the reciprocal extension ratio (λ). σ_{eng} is the nominal tensile stress ($\sigma_{eng} = f/A_0$, test force divided by the initial cross-sectional area of sample); the extension ratio λ is the ratio of deformed and initial length ($\lambda = l/l_0$); C_1 and C_2 are adjustable parameters. C_1 is related to crosslinking density, obtained from the Mooney–Rivlin equation's intercept. According to topological constraints of junction fluctuations theory in polymer networks,[43,44] the phenomenological C_2 term of the Mooney–Rivlin equation is related to physical entanglement of the polymer networks, which can be obtained from the Mooney–Rivlin equation's slope.

As shown in Figure 5, stress–strain curves are plotted as $\frac{\sigma_{eng}}{\lambda-1/\lambda^2}$ against $1/\lambda$ of all samples. Also, the plot was divided into three stages, in the initial strain region of $0.95 < \lambda < 1$, REACs exhibit universal elasticity, and then, Mooney–Rivlin curves converted gradually to be almost horizontal, which meant strain should be attributed to chemical crosslinking networks and physical entanglement in the high-strain region ($\lambda < 0.8$). However, in the low-strain region (Fig. 5, $0.95 > \lambda > 0.8$), slopes (C_2) of Mooney–Rivlin curves were not a fixed value but decreased quickly with strain, which implied that the essential of the REAC's large elongation was incarnated not only in physical entanglement networks between epoxy cured maleated asphalt and epoxy cured AA and MeHHPA but also in some other reasons.

The reason may be of the filler effect of asphalt or properties of asphalt itself. First, the original Mooney–Rivilin equation only considered physical entanglements of networks and chemical crosslinking networks, not including the influence of inactive stiffness fillers added. In this case, the strain amplification factor V, which was derived from Guth equation,[45,46] was used to take into account.

$$V = 1 + 2.5\varphi + 14.1\varphi^2,$$

where φ is the inactive stiffness filler volume concentration. The modified extension ratio Λ of filled rubber-likes should be calculated by the following equation:

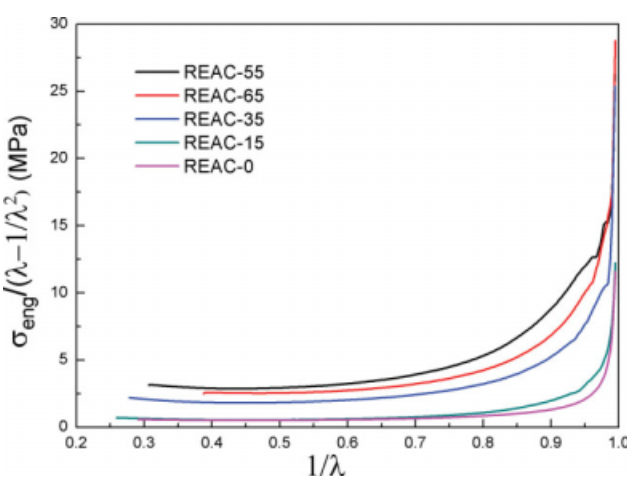

Figure 5 Mooney–Rivlin relations of REACs. [Color figure can be viewed in the online issue, which is available at www.interscience.wiley.com].

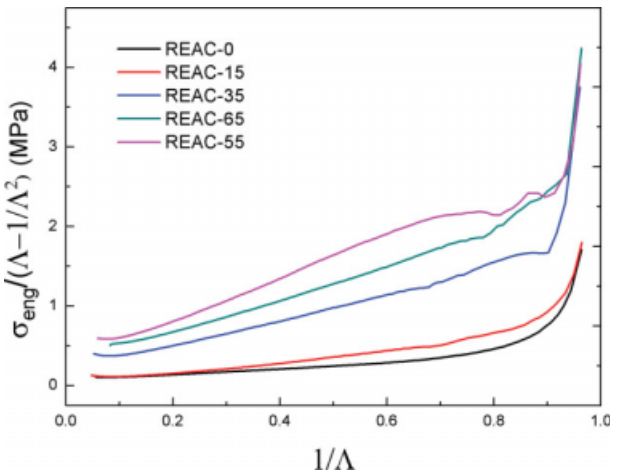

Figure 6 Modified Mooney–Rivlin relations of REACs. [Color figure can be viewed in the online issue, which is available at www.interscience.wiley.com].

$$\Lambda = 1 + V\varepsilon.$$

With the use of the strain amplification factor V, the Mooney–Rivlin graphs have been replotted in terms of $(\frac{\sigma_{eng}}{\Lambda-1/\Lambda^2})$ versus Λ (Fig. 6).

As shown in Figure 6, the modified Mooney–Rivlin equations are reduced to linear forms for all types of specimens in the high-strain region ($\Lambda <$ 0.8), which demonstrates that physical entanglement and chemical crosslinking networks are effected simultaneously in this region. It validated the judgment from the original Mooney–Rivlin equation. Furthermore, in the case of REACs, the intercepts of tensile curves increased with $C_{\text{maleated asphalt}}$, which is attributed to the increase of the density of chemical crosslinking networks. Also, Figure 6 shows C_1 values of maleated asphalt/epoxy composites are higher than that of unmaleated one because the addition of MAH introduced additional asphalt–asphalt and asphalt–epoxy networks.

However, as for the region of strain between $0.8 < \Lambda < 0.95$ (Fig. 6), the modified Mooney–Rivilin model cannot explain well. Therefore, viscoelasticity of asphalt, which is highly related to change of temperature, have to be considered to understand the nature of high elongation. Accordingly, experiments were performed at low and high temperature, respectively.

As shown in Figure 7, asphalt's viscoelasticity effect was obvious when tensile strength was loaded. At high temperature, the viscous flow state asphalt begins to intermolecule slip and cannot resist deformation any more. Although the chemical crosslinking networks and physical entanglements of REACs are still worked, they are also weak. Therefore, the deformation of REAC-55 is linear [Fig. 7(a)] with ε_b as high as 225%, σ as low as 0.5 MPa at 150°C. Although at low temperature, almost all the chain segments were frozen, the REACs would be "hard" with σ as high as 20.4 MPa [Fig. 7(b)]. However, asphalt itself has large "intermolecule free volumes"[47] to adapt shrinkage when cooled down; thus, REACs exhibited good elasticity with ε_b as high as 5.9% at −40°C.

After considering the combined analytical data, we propose that the REACs structures, depicted graphically in Figure 8, were formed as follows: first, some of the asphalt was maleated [Fig. 8(**I**)]; then, the unmaleated asphalt was attached with maleated asphalt [Fig. 8(**II**)] by the mechanical agitating and dispersing; when the curing agents AA and MeHHPA were added, they formed a kind of homogeneous phase (colloid) structure macroscopically [maleated asphalt as a kind of compatilizer, Fig. 8(**III**)]. Nevertheless, these curing agents with maleated asphalt and the bulk of the asphalt colloid formed sea-tideland-island colloid structures on a microscope scale, consisting of continuous sea of curing agents, dispersed island phase of asphalt, and in-between tideland of maleated asphalt. The sea-tideland-island morphology observed in the microscope image is latently formed in component **A** (Fig. 9).

As the curing agents' sea and maleated asphalt tideland are cured by the component **B** simultaneously, 3D thermosetting simultaneous interpenetrating networks (SIN) [Fig. 8(**IV**)] structure was formed. The density of crosslinking networks varies with $C_{\text{maleated asphalt}}$ and naturally increases with $C_{\text{maleated asphalt}}$. When $C_{\text{maleated asphalt}}$ is very low, the density of crosslinking networks should be relatively weak, as also confirmed by direct tensile test (Fig. 3, REAC-15).

The tensile deformation of REACs, with three stages (Fig. 3), is explicable in terms of the proposed

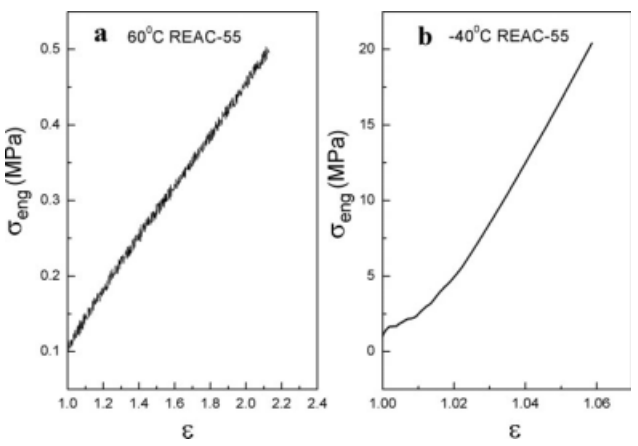

Figure 7 Stress–strain curves of REAC-55 at −40°C and 60°C.

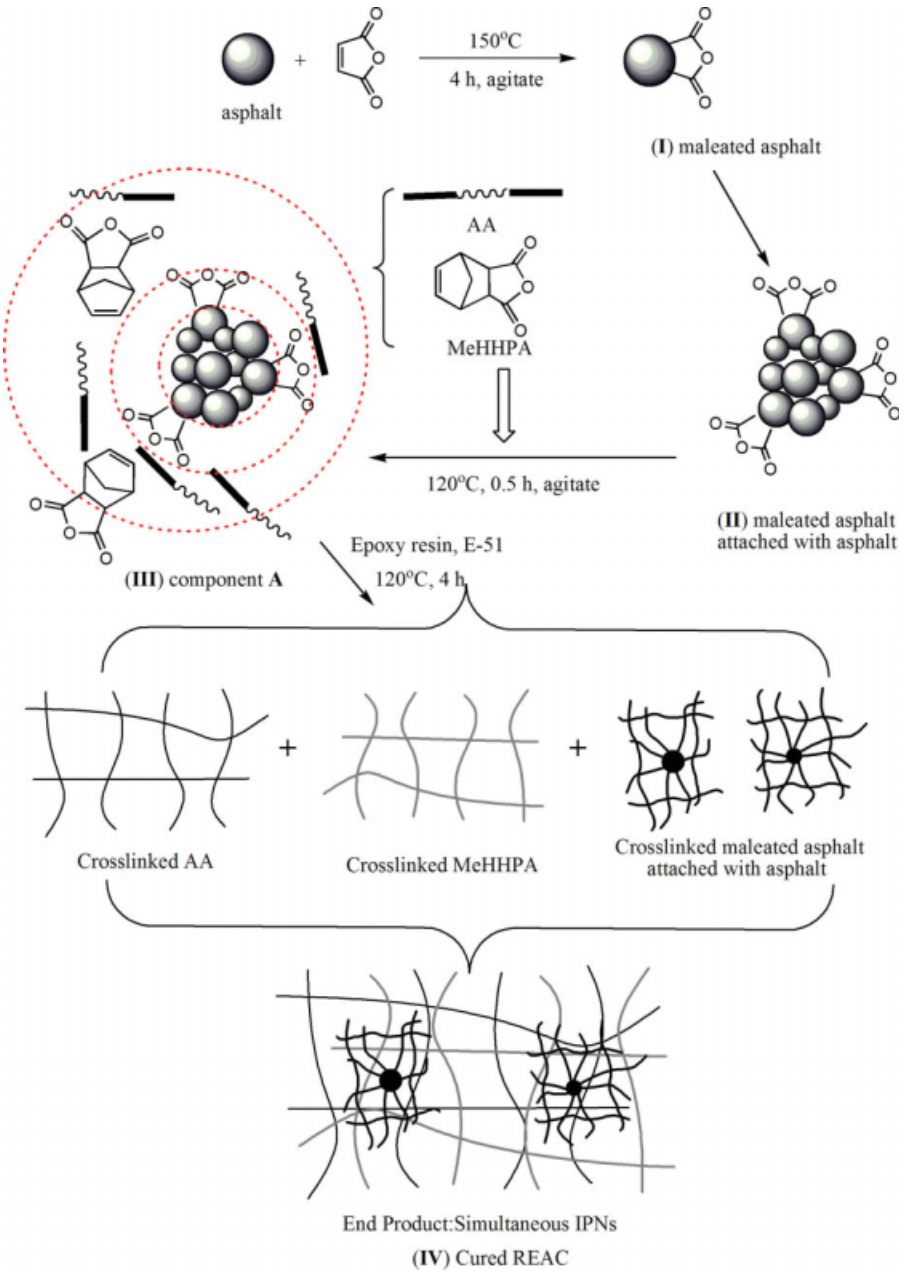

Figure 8 Scheme of the formation process of REACs. [Color figure can be viewed in the online issue, which is available at www.interscience.wiley.com].

model for the REACs depicted in Figure 8(**IV**). The first, low-strain region (I) with high modulus may correspond to the change of bond length and bond angle. When the stress increased beyond some critical value, the entanglements of networks began to deform gradually, in accordance with the region (II). The neighbored large deformation (stage III) should be attributed to tensile of chemical crosslinking networks to some degree accompanied by viscous deformation of asphalt colloid.

The high elongation and tensile strength observed in REACs are attributable to two main factors. One is the "hard" asphalt colloid. If there is no hard asphalt, for example, when asphalt is in the viscous flow state, the epoxy networks will be easy to rupture. It happens at high temperature (Fig. 7). The other is the formation of a SIN crosslinking networks structure between curing agents systems and maleated asphalt. In the case of REACs, the long-chain curing agents of AA (functionality = 2) and MeHHPA (functionality = 2) and short-chain maleated asphalt (functionality > 2) react with epoxy resin E-51, which formed local-high-global-low density crosslinking bimodal networks. If there is no

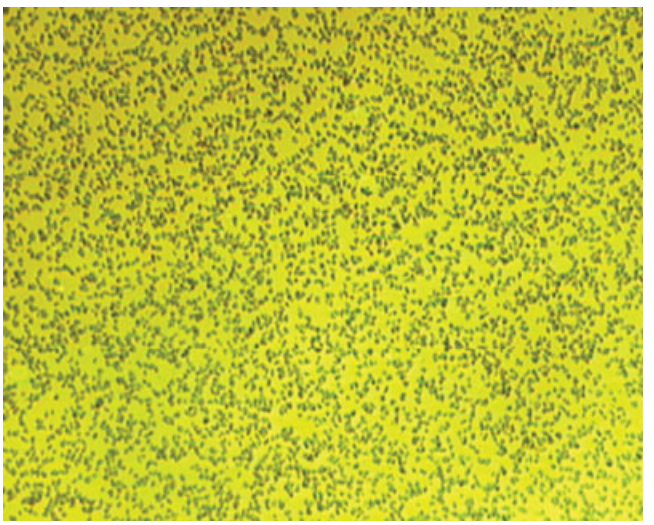

Figure 9 Microstructure of component **A**. [Color figure can be viewed in the online issue, which is available at www.interscience.wiley.com].

local-high density of crosslinking to bear the loaded stress, the REACs will be soft or even difficult to be cured, which happened in REAC-0 and control experiment without asphalt. If the local crosslinking density is higher than some critical value, the elongation and intensity will be changed to decrease (Fig. 3, REAC-60), and if the global crosslinking density is high, the high elongation will not exist like other traditional cured epoxy resins.[48–50]

CONCLUSIONS

In conclusion, we have prepared and characterized novel REACs with high elongation and tensile strength, consisting of cured short-chain maleated asphalt and long-chain curing agents of AA and MeHHPA with epoxy resin E-51. The mechanical properties of REACs could be controlled, in terms of ultimate strength, Young's modulus, and elongation at break, by altering the maleated asphalt content ($C_{\text{maleated asphalt}}$). The fracture energy of REACs was times higher than epoxy/(unmaleated asphalt) composite. Also, REACs show phenomena of critical mechanical conversion when $C_{\text{maleated asphalt}} > 55\%$. All the mechanical characteristics are totally distinct from those of cured conventional epoxy composites and asphalt or modified asphalt. Moreover, REACs exhibit atypical yielding behaviors and no-necking phenomena distinguishing them from previous materials. These characteristics of REACs were ascribed to the formation of a unique asphalt-filled "local-high-global-low" density crosslinking bimodal network morphology, consisting of cured maleated asphalt short-chain crosslinkings, cured AA and MeHHPA long-chain crosslinkings, and wherewith filled asphalt colloid. As REACs could be prepared in forms of films, sheets, rods, columns, and hollow tubes, they provide a new type of soft composites useful for advanced research and technologies, such as in civil, electric, or electronic engineering.

References

1. Zhang, K.; Wang, L.; Wang, F.; Wang, G.; Li, Z. J Appl Polym Sci 2004, 91, 2649.
2. Takashima, T. U.S. Pat. 2007/0,015,885 A1 (2007).
3. Yang, G.; Fu, S. Y.; Yang, J. P. Polymer 2007, 48, 302.
4. Wang, R.; Hao, C.; Chen, Z.; Yang, G.; Xia, Y.; Wang, J.; Fu, S. Acta Mater Compos Sin 2008, 25, 7.
5. Pearson, R. A.; Yee, A. F. Polymer 1993, 34, 3658.
6. Bhuniya, S.; Adhikari, B. J Appl Polym Sci 2003, 90, 1497.
7. Wen, G.; Zhang, Y.; Zhang, Y.; Sun, K.; Fan, Y. Polym Test 2002, 21, 295.
8. Lu, X.; Isacsson, U. Polym Test 2001, 20, 77.
9. Sinan, H.; Emine, A. Mater Lett 2004, 58, 267.
10. Perez-Lepe, A.; Martinez-Boza, F. J.; Gallegos, C. Energy Fuels 2005, 19, 1148.
11. Lu, X.; Isacsson, U.; Ekalad, J. Mater Struct 2003, 264, 652.
12. Becker, M. Y.; Muller, A. J.; Rodriguez, Y. J Appl Polym Sci 2003, 90, 1772.
13. Polacco, G.; Stastna, J.; Biondi, D.; Antonelli, F.; Vlachovicova, Z.; Zanzotto, L. J Colloid Interface Sci 2004, 280, 366.
14. Polacco, G.; Stastna, J.; Vlachovicova, Z.; Biondi, D.; Zanzotto, L. Polym Eng Sci 2004, 44, 2185.
15. Yu, J.; Cong, P.; Wu, S. J Appl Polym Sci 2009, 6, 3557.
16. Yu, J.; Cong, P.; Wu, S.; Cheng, S. J Wuhan Univ Tech (Mater Sci Ed) 2009, 24, 462.
17. Çubuk, M.; Gürü, M.; Çubuk, M. K. Fuel 2009, 7, 1324.
18. Hayashi, S.; Isobe, M.; Yamashita, T. U.S. Pat. 4,139,511 (1979).
19. Gallagher, K. P.; Vermilion, D. R. U.S. Pat. 5,576,363 (1996).
20. Gallagher, K. P.; Vermilion, D. R. U.S. Pat. 5,604,274 (1997).
21. Sasada, Y.; Hagiwara, A.; Fuji, M.; Takeuchi, K.; Ueno, S.; Kanazawa, T.; Ikeda, T. WO. Pat. 2007023833-A1 (2007).
22. Santos, Fabio. WO. Pat. 2007/131312 A2 (2007).
23. Mechin, F.; Pascault, J.; Lambour, S.; Ferrand, J. U.S. Pat. 2004/0,030,026 A1 (2004).
24. Wu, W. W. L.; Stamp, J. R.; Brothers, W. J. U.S. Pat. 6,964,626B1 (2005).
25. Boucher, J. J.; Wang, I. H.; Romine, R. A. Am Chem Soc, Div Pet Chem Prepr 1990, 35, 556.
26. Herrington, P. R.; Wu, Y.; Forbes, M. C. Fuel 1999, 78, 101.
27. Kang, Y.; Chen, Z.; Min, Z.; Huang, W.; Cheng, G.; Wang, X. J Southeast Univ (Natural Sci Ed) 2006, 36, 308.
28. Mark, J. E. J Phys Chem B 2003, 107, 903.
29. Viers, B. D.; Mark, J. E. J Inorg Organomet Polym Mater 2007, 17, 283.
30. Wu, S. Z.; Mark, J. E. Polym Rev 2007, 47, 463.
31. Mishra, V.; Murphy, C. J.; Sperling, L. H. J Appl Polym Sci 1994, 53, 1425.
32. He, M. J.; Chen, W. X.; Dong, X. X. Polymer Physics (Revision); Fudan University Press: Shanghai, China, 1990. p 301.
33. Kreitmeier, S.; Wittkop, M.; Wagner, T.; Goritz, D.; Zietz, R. Colloid Polym Sci 1995, 273, 1008.
34. LiQiang, S.; Zhikang, X.; Youyi, X. J Appl Polym Sci 2002, 84, 203.
35. Chunhui, D.; Baoku, Z.; Youyi, X. J Zhejiang Univ (Eng Sci) 2006, 40, 1.
36. Miles, M. J.; Baer, E. J Mater Sci 1979, 14, 1254.
37. Kloczkowski, A. Polymer 2002, 43, 1503.
38. Rubinstein, M.; Panyukov, S. Macromolecules 2002, 35, 6670.

39. Drozdov, A. D. Int J Solids Struct 2007, 44, 272.
40. Lu, L.; Zhai, Y.; Zhang, Y.; Ong, C.; Guo, S. Appl Surf Sci 2008, 255, 2162.
41. Bokobza, L. J Appl Polym Sci 2004, 93, 2095.
42. Bhattacharyya, S.; Sinturel, C.; Bahloul, O.; Saboungi, M.; Thomas, S.; Salvetat, J. Carbon 2008, 46, 1037.
43. Rubinstein, M.; Colby, R. H. Polymer Physics; Oxford University Press: New York, 2003; p 164.
44. Klüppel, M.; Schramm, J. Macromol Theory Simul 2000, 9, 742.
45. James, H. M.; Guth, E. J Appl Phys 1944, 15, 294.
46. Bokobza, L. Macromol Mater Eng 2004, 289, 607.
47. Nishijima, S.; Honda, Y.; Okada, T. Cryogenic 1995, 35, 779.
48. LeMay, J. D. Structure and Ultimate Properties of Epoxy Resins. Advances in Polymer Science 78; Springer-Verlag: Berlin Heidelberg, 1986.
49. Sui, G.; Jana, S.; Salehi-khojin, A.; Neema, S.; Zhong, W.; Chen, H.; Huo, Q. Macromol Mater Eng 2007, 292, 467.
50. Njuguna, J.; Pielichowski, K.; Alcock, J. R. Adv Eng Mater 2007, 9, 835.